

Photonic logic by linear unidirectional interference

Pavel Ginzburg, Alex Hayat, Victoria Vishnyakov and Meir Orenstein

EE Department, Technion, Haifa 32000, Israel
gpasha@tx.technion.ac.il

Abstract: A novel concept of unidirectional optical interference is presented, inspired by a non-Hermitian formulation of quantum mechanics via Maxwell-Schrödinger equation analogy. This model is employed for the design of photonic devices controlling strong fields by weak ones, suitable for large-scale optical logic. Implementations of very low-power photonic logic based on linear unidirectional optical gratings are presented. A linear photonic inverter is demonstrated and its performance is optimized by numerical calculations. The simulations are performed by full-vectorial beam propagation methods showing high signal to noise ratios.

©2009 Optical Society of America

OCIS codes: (200.4660) Optical logic; (130.4815) Optical switching devices; (000.1600) Classical and quantum physics

References and links:

1. Z. Li, and G. Li, "Ultrahigh-speed reconfigurable logic gates based on four-wave mixing in a semiconductor optical amplifier," *IEEE Photon. Technol. Lett.* **18**, 1341-1343 (2006).
2. E. Shumakher, A. Hayat, A. Freimain, M. Nazarathy, G. Eisenstein, "Timing Extraction of a 10-gb/s NRZ Signal Using an Electro-Optic Multiplication Scheme," *IEEE Photon. Technol. Lett.*, **16**, 2353 (2004).
3. J. Wang, J. Sun, and Q. Sun, "Experimental observation of a 1.5 μm band wavelength conversion and logic NOT gate at 40 Gbit/s based on sum-frequency generation," *Opt. Lett.* **31**, 1711-1713 (2006).
4. T.K. Liang, L.R. Nunes, M. Tsuchiya, K.S. Abedin, T. Miyazaki, D. V. Thourhout, W. Bogaerts, P. Dumon, R. Baets, and H.K. Tsang, "High speed logic gate using two-photon absorption in silicon waveguides," *Opt. Commun.* **265**, 171-174 (2006).
5. X. Zhang, Y. Wang, J. Sun, D. Liu, and D. Huang, "All-optical AND gate at 10 Gb/s based on cascaded single-port-couple SOAs," *Opt. Express* **12**, 361-366 (2004).
6. Y. J. Jung, J. Park, and N. Park, "Wavelength-transparent nonlinear optical gate based on self-seeded gain modulation in folded tandem-SOA," *Opt. Express* **15**, 4929-4934 (2007).
7. P. Ginzburg, and M. Orenstein, "Photonic switching in waveguides using spatial concepts inspired by EIT," *Opt. Express* **14**, 11312-11317 (2006).
8. S. E. Harris, "Electromagnetically induced transparency," *Phys. Today* **50**, 36-42 (1997).
9. M. Greenberg and M. Orenstein, "Unidirectional complex grating assisted couplers," *Opt. Express* **12**, 4013-4018 (2004).
10. C. M. Bender, "Making sense of non-Hermitian Hamiltonians," *Rep. Prog. Phys.* **70**, 947-1018, (2007).
11. C. M. Bender, J.-H. Chen, and K. A. Milton, "PT-Symmetric Versus Hermitian Formulation of Quantum Mechanics," *J. Phys. A: Mathematical and General* **39**, 1657-1668 (2006).
12. R. El-Ganainy, K. G. Makris, D. N. Christodoulides, and Z. H. Musslimani, "Theory of coupled optical PT-symmetric structures," *Opt. Lett.* **32**, 2632-2634 (2007).
13. S. Klaiman, U. Gunther, and N. Moiseyev, "Visualization of Branch Points in PT-Symmetric Waveguides," *Phys. Rev. Lett.* **101**, 080402 (2008).
14. M. O. Scully, and M. Fleischhauer, "Lasers Without Inversion," *Science* **263**, 337 (1994).
15. A. Hayat, E. Small, Y. Elor, and M. Orenstein, "Phasematching in Semiconductor Nonlinear Optics by Linear Long-Period Gratings," *Appl. Phys. Lett.* **92**, 181110 (2008).
16. D. Marcuse, *Theory of Dielectric Optical Waveguides*, 2nd ed. (Academic, New York, 1991).
17. M. Greenberg, and M. Orenstein, "Optical Unidirectional devices by Complex Spatial Single Sideband Perturbation," *IEEE J. of Quantum Electron.* **41**, 1013-1023 (2005).
18. M. Greenberg, and M. Orenstein, "Irreversible coupling by use of dissipative optics," *Optics Lett.* **29**, 451-453, (2004).
19. W. Huang, C. Xu, S. Chu, and S. Chaudhuri, J., "The finite-difference vector beam propagation method: analysis and assessment," *J. Lightwave Technol.* **10**, 295-305 (1992).

1. Introduction

A large variety of non-linear optical devices for all-optical logic systems have been investigated. One can identify two main trends in optical switching. The first is employing passive nonlinear optical media, e.g. $\chi^{(3)}$ based effects [1], electro-optical multiplication [2], sum frequency generation [3], and two-photon absorption [4]. The second is based on gain nonlinearity of active devices, such as cross gain modulation [5] and self-seeded gain modulation [6].

For large-scale integration, efficient, robust, low-power all-optical logic devices are required. However the relatively weak nonlinear effects employed, significantly limit the efficiency of the devices. Moreover, as the integrated logic is expected to continue shrinking and to consume negligible power, employing nonlinear effects for optical logic will become much less practical. Photonic switching devices based on linear optics are, therefore, crucial for future large-scale optical computing. In a previous work [7] we presented a bidirectional interferometric scheme, inspired by the reversible Electromagnetically Induced Transparency (EIT) [8], for linear switching within a waveguide by coupling between the guided modes using two linear gratings. Destructive and constructive interference between the modes provides the switching characteristics. The main impediment in such interferometric switches is the high sensitivity to device dimensions and amplitude-comparable signals, which prevent large signal-to-noise ratio and cascadability. The fundamental limiting factor of bidirectional interferometric devices is the underlying space (time) reversibility of Maxwell (Schrödinger) wave equation.

Here we present optical logic elements based on linear optics and employing two mechanisms related to analogies from quantum mechanics: EIT and unidirectionality [9] closely related to non-Hermitian (complex) potentials in Quantum Mechanics (QM). While in conventional QM time reversibility may be broken by a magnetic field, the best candidates in photonics are gain/loss processes, such as periodic loss/gain gratings coupled to index gratings [9]

The use of complex gratings allows not only switching of optical signals by amplitude-comparable signals, but also enables switching “strong” signals by much weaker ones, important for fan-out and large-scale integration. Another significant advantage of unidirectional devices is their robustness to device length inaccuracies, in contrast to index-only gratings that must have very precise lengths due to power oscillations between the modes. A useful property of a unidirectional device is that the power of the switched signal is amplified during the switching process.

In Sec. 2 we convey the concept of unidirectional EIT, in Sec. 3 an optical inverter implementation and theory are presented. In Sec. 4 we present the simulation results and performance of such optical inverters.

2. Unidirectional EIT (UEIT) concept

Interferometric concepts, closely related to QM, introduce a breakthrough solution for linear (power-independent) schemes of interaction between two weak comparable-amplitude optical signals. The basic phenomenon of coherent EIT [8] provides the control over the absorption coefficient of a probe signal by a pump field of a different color and specific amplitude and phase relations. Rabi oscillations of the coherent-EIT scheme dictate the natural limit of the ratio between the probe and the pump amplitudes. Rabi oscillations stem from the Hermiticity of the time-dependent Hamiltonian of two-level systems, coupled to harmonic electromagnetic fields. Recently, non-Hermitian potentials have gained considerable interest in science, since they allow reformulating the basic postulates of quantum theory with less strict mathematical assumptions without, however, compromising the laws of nature [10, 11], and optical analogs were studied in configuration of gain/loss waveguides uniform in the mode propagation direction [12,13].

Here we consider a unidirectional Rabi flip which, as far as we know, was not considered before. Rabi flip is defined as the electromagnetic interaction of coupling between two energy

levels unidirectionally (Fig. 1). (i.e. an electron can undergo a transition from the first level to the third, but *not* vice versa). A similar situation was shown to exist in inversionless lasers [14]. We study the quantum mechanical scheme of coherent unidirectional EIT (UEIT).

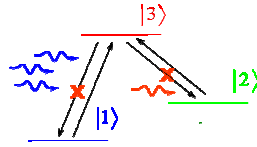


Fig. 1. Unidirectional EIT λ -scheme. The forbidden transitions are crossed.

UEIT enables the control of the transparency condition of a strong field by a weak one, employing a strong dipole moment between the corresponding quantum levels, which is impossible in bidirectional (conventional) coherent EIT schemes [7].

We study optical-waveguide mode analogue of UEIT, using the analogy between the Schrödinger and the transverse-electric field Maxwell wave equations. Here the optical modes replace the wave-functions, while the periodical gratings replace time-harmonic electromagnetic fields and mode propagation acts as time evolution of the quantum eigenstate.

While a purely real refractive index grating has both positive and negative components of momentum coupling between modes in a space-reversible manner – namely - bidirectional [15, 16], a complex grating can have only one-directional momentum component [9, 17, 18]. Therefore, beating between modes typical to waveguides with real gratings will not occur in a well-designed complex one, resulting in a unidirectional power transfer.

3. Theoretical background and optical logic implementation

Here we theoretically demonstrate a possible implementation of an inverter and propose a way to construct a NAND gate – which can span a complete set of logical operations.

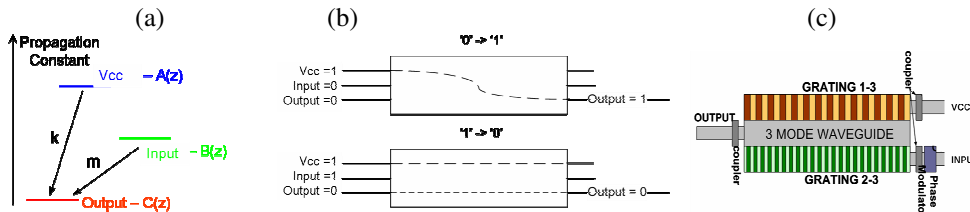


Fig. 2. Optical Inverter (a) Mode diagram with appropriate unidirectional gratings and their strength m and k . (b) Block diagram of the inverter (c) Inverter's implementation schematics.

Our photonic logic concept is based on complex double-period (for invertors) and triple-period (for NAND gates) gratings in a dielectric waveguides. The optical inverter is realized by a three-mode slab waveguide (three level atom in QM) with embedded two complex gratings (pump and probe fields in QM): one with a period matching the propagation constant difference between the fundamental mode (“the powering channel -Vcc”) and the third mode (“Output”), and the other matching the difference between the third mode and the second mode (“Input”) (Fig. 2(a)). Unidirectional coupling takes place from the Vcc to the Output and from the Input to the Output. When a logic '1' is present in the Input (power is launched into the second mode) the power is transferred both from the Vcc and the Input to the Output (the 'bright state' in QM EIT). If the Vcc - Input relative phase is prepared to be π there will be no power on the Output (logical '0') due to the destructive interference between the modes ('dark state' in QM EIT). When the Input is '0' (no power launched to the second mode) power is transferred from the Vcc to the Output which results in logic '1' (Fig 2(b)). The device is unidirectional since there will be no power transfer from the Output mode to the

Input or the Vcc modes. For cascability - the Output of the inverter which is the third optical mode may be converted by an additional passive coupler to the second mode in order to be launched into the Input of the following stage.

The analysis of modal propagation (QM time evolution) in the interaction regime can be performed by the coupled mode theory [16]. The “weak” grating assumption assists in selecting only the resonantly coupled modes and enabling the integration of the amplitude over a grating period due to small changes (slowly varying amplitudes - quantum-mechanically - resonant transitions in secular approximation). A , B and C are the respective complex amplitudes (electron occupation amplitudes in QM EIT) of the Vcc, Input, and Output modes:

$$\partial_z A = 0 \quad \partial_z B = 0 \quad \partial_z C = jkA + jmB \quad (1)$$

where k and m are the Vcc-Output and Input-Output coupling coefficients respectively (Fig. 2(a)). Applying the following initial conditions on the amplitudes of the Vcc and input modes (1st and 2nd mode respectively) and no output power (3rd mode):

$$A(0) = A_0 \quad B(0) = B_0 \quad C(0) = 0 \quad (2)$$

The solution of Eq. given Eq. 2 is:

$$A(z) = A_0 \quad B(z) = B_0 \quad C(z) = jkA_0 z + jmB_0 z \quad (3)$$

The initial amplitude of the Input $B(0) = B_0$ will determine the Output of the device (‘0’ or ‘1’). If $B(0) = 0$ the Output will grow linearly with z and will reach the level ‘1’. If $B(0) = 1$ and there is a phase difference of π ($kA_0 = -mB_0$) the output will be ‘0’ for all z . The phase sensitivity of the device will be discussed in section 4. It can also be seen that the grating coupling strength (k and m) has to be chosen to match the ratio between the Vcc and Input amplitudes so that C will vanish for all z . On the other hand, this condition allows the improvement of Vcc to Input ratio. Choosing $m > k$ allows using weak input signal $B_0 < A_0$.

A NAND gate can be realized similarly but using a four-mode waveguide (four-level atom in QM) with three unidirectional gratings (Fig. 3). The structure will require one grating to couple the Vcc to the Output and 2 “weaker” grating (theoretically $\frac{1}{2}$ the strength of the first for same amplitude signals) to couple between the two Input signals and the Output. For an Input amplitude weaker than the Vcc amplitude, the 2 gratings which couple the gates to the Output have to be stronger than the 1st grating to compensate for the amplitude difference.

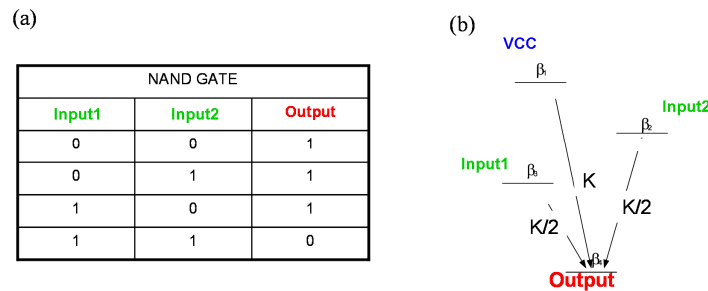


Fig. 3. Optical NAND (a) logic table (b) Mode diagram with unidirectional gratings and their strength $k/2$ and k .

Here we present the concept for the simple case of comparable amplitudes. The device has four possible states: when both Inputs are ‘0’ the Vcc is coupled to the Output with no interruption. If one of the Inputs is ‘1’, due to the phase difference between the signal and the part of the Vcc, the Input will be transferred to the Output, resulting in a reduced but yet non-zero output. Only when both Inputs are ‘1’, the destructive interference will result in no Output signal.

The implementation of a double (triple) complex grating device is quite involved. Schematically, the device has to be implemented in a gain medium waveguide (e.g.

semiconductor amplifier) while each grating is formed by a periodic current injection (to generate the imaginary – gain/loss grating) while the real part (which should be $\pi/2$ shifted in respect to the gain/loss part) is implemented either by etched grating structure [15] or dynamically by applying a periodic voltage on the intrinsic layer of the semiconductor employing the electro-optic effect (Fig. 4). Realizing multiple gratings can be better performed by using 3(4) coupled waveguides – rather than the 3(4) modes – allowing each of the gratings to be implemented on the top of a separate guide.

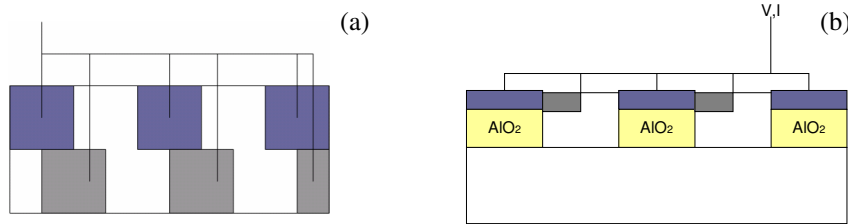


Fig. 4. Device implementation proposal (a) Top view (b) Side View

4. Simulation results and performance

To validate the results, such a waveguide device was simulated, using a full-vectorial beam propagation method (FVBPM) [19]. The interaction region is comprised of a typical AlGaAs-based slab waveguide having a core refractive index $n_{core}=3.3$ surrounded by $n_{clad}=3.1$; the core width is $2\mu\text{m}$ and the length is $500\mu\text{m}$ (~ 40 grating periods). The waveguide supports 3 guided modes at $\lambda_0=1.55\mu\text{m}$. Two spatial sinusoidal gratings with refractive index modulation ($\sim 0.1\%$ depth) and periods matching the inter-modal propagation constant differences were imposed on the waveguide core (Fig. 5(a)).

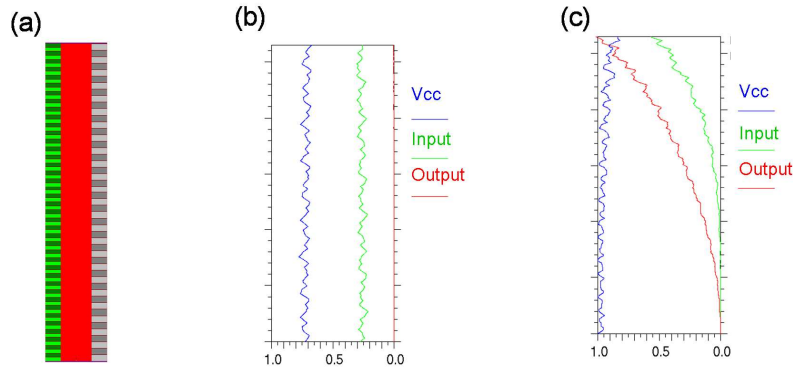


Fig. 5. Simulation results (a) Schematic top view of the simulated device; Total electric field amplitude and the power at the three modes are depicted for (b) "1->0" – Input signal, no Output signal. (c) "0->1" – no Input signal, Output signal

The system's steady state ('1' to '0') appears on Fig. 5(b), while Fig. 5(c) represents the '0' to '1' switching. The slight amplitude fluctuations of the modes are caused by deviations from the slowly varying field approximation.

The extinction ratio (on/off power for optical inverter and transparency/absorption) of the device is 40dB for the $500\mu\text{m}$ long device and is dependent on the device's length. The Phase sensitivity was calculated to be manageable: 10% error in the input phase causes 15% difference on the output signal. The inverter characteristic graphs are represented on Fig. 6 for two different device lengths – $500\mu\text{m}$ and $1000\mu\text{m}$. It can be seen that the longer the device, the larger Vcc to Input ratio can be achieved due to the amplification of the signal. The shorter device exhibits Vcc to Input ratio of $\sim 2-3$ (Fig 6(a)), while for longer device the ratio is $\sim 5-6$

(Fig 6(b)). V_{cc} to Input ratio and other performance parameters such as the maximal Input noise are tunable per design by defining “noise margin limits”.

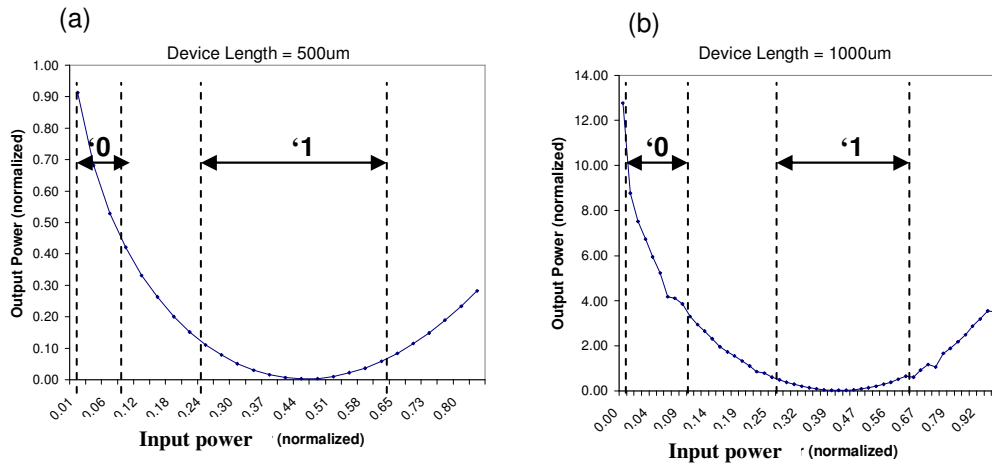


Fig. 6. Normalized output power as a function of normalized input power. Noise margin limits are marked (a) Device length 500µm, fan-out ~2-3 (b) Device length 1000µm, fan-out ~5-6.

The maximal frequency of the device operation is determined by the optical signal propagation time. For a 1000µm long device, the propagation time is about 10psec making the maximal frequency near 100GHz. Spontaneous emission in the gain regions is a source of noise in such active devices. The spontaneous emission related noise power for the simulated device at 100GHz operation rate (the relevant bandwidth) and into the relevant mode was calculated to be less than a 100pWatts. For the requirement that the spontaneous emission noise will be negligible in comparison to the noise allowed on the Input, it should be in the order of a nWatt. For a given V_{cc} to Input ratio, the minimal V_{cc} power that can be used is determined by this requirement. For the simulated device, the ratio is ~5-6, and thus the minimal V_{cc} power is ~5nWatts. A trade-off exists between the maximal V_{cc} to Input ratio and the operation voltage (current) – the longer the device the better is the fan-out but also the stronger the spontaneous emission is, which determines the minimal operation voltage. Operation in such a low power regime is not reported in any of the existing implementations of optical logic to the best of our knowledge.

5. Summary

We have demonstrated the concept of UEIT inspired by non-Hermitian QM and employed it for photonic inverter implementation using linear unidirectional optics. The concept may be extended to achieve large-scale photonic logic, integrable into semiconductor circuits. Simulation results show possible operation at 100Ghz, with signal strength on the order of nWatts. The proposed device is robust to its physical dimensions due to the non-periodical unidirectional behavior of optical power transfer between the different modes. Furthermore, the UEIT-based scheme allows the possibility of strong optical signal manipulation by a weak one.